

# Dynamics of Large Semiflexible Chains Probed by Fluorescence Correlation Spectroscopy

D. Lumma,<sup>1</sup> S. Keller,<sup>2</sup> T. Vilgis,<sup>1</sup> and J. O. Rädler<sup>2</sup>

<sup>1</sup>Max-Planck-Institut für Polymerforschung, Ackermannweg 10, D-55128 Mainz, Germany

<sup>2</sup>Ludwig-Maximilians-Universität, Geschwister-Scholl-Platz 1, D-80539 München, Germany

(Received 9 December 2002; published 30 May 2003)

Fluorescence correlation spectroscopy was used to probe the dynamics of  $\lambda$ -phage DNA in aqueous solution labeled with the randomly intercalating dye TOTO. The linear macromolecules (i) carry more than one chromophore and (ii) are larger than the waist of the focal volume. The correlation function decays significantly faster than expected for a stiff globule of corresponding size but is in good agreement with the dynamic model of semiflexible chains including hydrodynamic interactions. As the chromophore density is lowered the correlation time decreases in accordance with this model.

DOI: 10.1103/PhysRevLett.90.218301

PACS numbers: 83.10.Mj, 87.14.Gg, 87.15.Ya, 87.64.Tt

Fluorescence correlation spectroscopy (FCS) has become an important tool for investigating the dynamic properties of single molecules in solution [1]. The method is based on detecting the fluctuations of the fluorescent light intensity in a small and fixed volume element, usually formed by a laser focus of submicron waist size. FCS has found widespread application to partially labeled, biological materials, probing diffusive behavior [2,3], reaction kinetics [4], or intracellular protein concentrations [5]. The theoretical framework of FCS has thus far focused on the diffusion of pointlike particles smaller than the focal volume. With growing interest in colloidal systems [6], the method has been extended to the diffusion of particles with a finite size, exceeding the diameter of a laser focus [7]. A more complex dynamic problem arises when biological macromolecules are investigated which are both significantly larger than a laser focus and labeled with more than one chromophore. Reports of FCS measurements on macromolecules are rare [8,9] and have thus far not considered any internal degrees of polymer dynamics.

This Letter presents an experimental study on the dynamics of randomly labeled  $\lambda$ -phage DNA [10] with a contour length of  $17\ \mu\text{m}$ , whose average end-to-end distance exceeds about 5 times the waist size of the laser focus employed. The essential features of our experiments are illustrated in Fig. 1. We investigate the partially correlated many-body motion of fixed, but randomly distributed, markers along a flexible linear chain. When the DNA is centered on the focus, on average only 1/3 of all markers are excited, as illustrated in Fig. 1(a). By successively decreasing the label density, we show that internal chain dynamics become increasingly visible in our autocorrelations, as for the case in Fig. 1(b). We compare the measured FCS autocorrelation with theoretical correlation functions derived from the dynamic structure factor of semiflexible polymers including hydrodynamic interactions [11].

$\lambda$ -phage DNA was purchased from MBI Fermentas (St. Leon-Rot, Germany). The intercalating dye TOTO-1

iodide (514/533) was purchased from Molecular Probes (Eugene, OR, USA). For all DNA solutions, a buffer containing 10 mM Tris at  $p\text{H} \approx 8.0$ , 10 mM sodium chloride, 1 mM EDTA, and 10 mM ascorbic acid in deionized water was used. DNA samples were diluted to 0.1 nM, slightly below a conservative estimate for the overlap concentration of  $c^* \approx 0.5\ \text{nM}$ . Label densities were adjusted between 1/6 and 1/8000 dye molecules per base pair ( $\text{bp}^{-1}$ ). Samples were gently shaken at room temperature for at least 1 h, avoiding any macroscopic inhomogeneities in dye concentration. The brightness of intercalating dyes drops drastically once unlocked from the DNA double strand [12], ensuring that our data are not influenced by freely diffusing dye.

The principles of FCS are described elsewhere [12]. Briefly, the technique studies the number fluctuations of labeled markers in an open volume on the order of  $10^{-15}\ \text{l}$ . The autocorrelation of a time-resolved

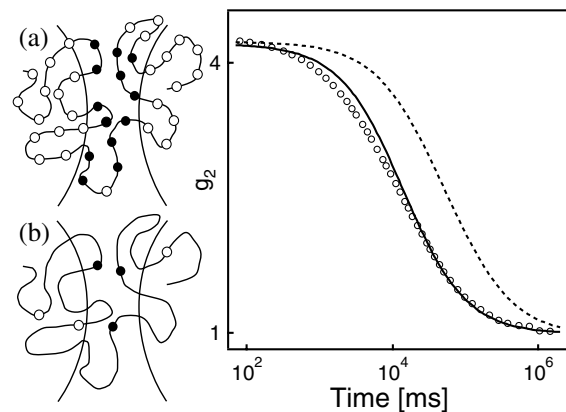


FIG. 1. The measured autocorrelation curve  $g_2$  for dilute  $\lambda$ -phage DNA deviates from the correlation function expected for a stiff finite-size polymer with  $R_g = 0.73\ \mu\text{m}$  (dashed line). The solid line shows the poor agreement with a best fit to the correlation function of a pointlike particle. The drawings illustrate labeled DNA as a chain of linked chromophores for (a) high and (b) low average label densities.

fluorescence signal permits the characterization of particle concentration and dynamics. We used a commercial setup by Carl Zeiss (Jena, Germany) consisting of the module Confocor 2 and the microscope model Axiovert 200 with a Zeiss C-Apochromat 40× NA 1.2 water immersion objective. For excitation, the 514 nm line of a 25 mW argon laser was used. Emitted fluorescence was detected at wavelengths longer than 530 nm by means of an avalanche photodiode enabling single-photon counting.

For calibration, an aqueous solution of 10 nM rhodamine 6G (R6G) was studied before each data acquisition series and fitted to the standard FCS correlation function

$$g_2(t) = 1 + g_{\text{tr}}(t)g_{\text{diff}}(t), \quad (1)$$

where  $g_{\text{tr}}(t) = [1 + e^{-t/\tau_{\text{tr}}}T/(1 - T)]$  denotes the triplet decay [13] and  $g_{\text{diff}}(t)$  denotes the three-dimensional (3D) Brownian diffusion of pointlike particles

$$g_{\text{diff}}(t) = N^{-1}[1 + (t/\tau_{\text{D}})]^{-1}[1 + t/(f^2\tau_{\text{D}})]^{-1/2} \quad (2)$$

where  $r_0$  is the waist size of the focus,  $z_0$  is its height,  $f = z_0/r_0$ , and  $\tau_{\text{D}} = 0.25r_0^2/D$  is the diffusion time that the particle dwells on average in the focus [1].  $N$  denotes the average number of marked objects in the effective focal volume. With the R6G diffusion constant  $D_{\text{R6G}} = 2.8 \times 10^2 \mu\text{m}^2 \text{s}^{-1}$  [12] as a reference, the focal waist size and shape parameter were determined ( $r_0 \approx 0.18 \mu\text{m}$  and  $f \approx 9$ ) and were used for all subsequently acquired data.

In order to describe the particle dynamics of flexible and extended objects, we derive the normalized FCS correlation function from the dynamic structure factor (intermediate scattering function)  $S(\vec{Q}, t)$  of the label distribution on the macromolecule. Following the seminal work by Rička and co-workers [6], we use

$$g_{\text{diff}}(t) = \frac{1}{N} \frac{\int \Phi(\vec{Q})S(\vec{Q}, t)d^3Q}{\int \Phi(\vec{Q})S(\vec{Q})d^3Q}, \quad (3)$$

where  $S(\vec{Q})$  denotes the static scattering factor, and  $\Phi(\vec{Q}) = (i_0^2/64)r_0^4z_0^2 \exp[-r_0^2(Q_x^2 + Q_y^2)/4 - z_0^2Q_z^2/4]$  a Gaussian filter function in reciprocal space that is derived from the real-space detection efficiency,  $i(\vec{r})$ , by Fourier transformation  $\Phi(\vec{Q}) = FT\{i(\vec{r})\}_{\vec{Q}} FT\{i(\vec{r})\}_{-\vec{Q}}$ . Hence FCS views the self-correlation function of the movement of tagged particles filtered through an experimental apparatus that is most sensitive around  $\vec{Q} = 0$ . Using  $S(Q, t) = \exp(-Q^2Dt)$  for Brownian diffusion of pointlike particles, Eq. (2) is regained from Eq. (3).

Figure 1 shows the FCS autocorrelation  $g_2$  for DNA chains with a label density of  $1/6 \text{ bp}^{-1}$ , corresponding to about 25 markers per DNA persistence length. In a first approach we model the DNA as a static Gaussian chain with form factor  $S_{\text{debye}}(Q^2R_g^2)$  and  $R_g$  the radius of gyration [14]. Using  $S(Q, t) \approx S_{\text{debye}}(Q^2R_g^2) \exp(-Q^2Dt)$  in Eq. (3) and enforcing  $R_g \approx 1.5R_h = k_B T/(4\pi\eta D)$  [15] with  $k_B T$  the thermal energy,  $\eta$  the buffer bulk viscosity,

we obtain the unsatisfactory dashed line. We used the value  $R_g = 0.73 \text{ m}$  for  $\lambda$ -phage DNA [10].

For comparison the full line represents the best fit to Eq. (2). This curve systematically deviates from the measured data at longer times and yields an apparent diffusion constant of  $D_{\text{FCS}} = 1.01 \pm 0.05 \mu\text{m}^2 \text{s}^{-1}$  or  $R_{\text{gFCS}} \approx 0.340 \pm 0.017 \mu\text{m}$ , which is significantly smaller than the values found in numerous other studies on  $\lambda$ -phage DNA. In particular, dynamic light scattering (DLS) obtained  $D_{\text{DLS}} = 0.41 \pm 0.05 \mu\text{m}^2 \text{s}^{-1}$  or  $R_{\text{gDLS}} = 0.837 \pm 0.102 \mu\text{m}$ , and fluorescence microscopy (FM) yields  $D_{\text{FM}} = 0.47 \pm 0.03 \mu\text{m}^2 \text{s}^{-1}$  or  $R_{\text{gFM}} \approx 0.730 \pm 0.047 \mu\text{m}$  [10]. This indicates that a faster process determines the number fluctuations in our observation volume. In fact, it is sensible to assume that internal conformational diffusion of the chain leads to fluctuations in the fluorescence intensity, especially when considering that the laser focus illuminates only a subvolume of the entire chain. In the following we support this picture by a more general ansatz [16] using a stretched-exponential form for the dynamic structure factor  $S(Q, t) = \exp[-Q^2(\gamma t)^\beta]$ . According to [17] we expect for the Rouse model  $\beta = 1/2$  and  $\gamma = kTb^2/\zeta$  and in the case of the Zimm model in the limit of large wave vectors  $\beta = 2/3$  and  $\gamma = kT/6\pi\eta_s$ . For the following the dynamic structure factor is more relevant for semiflexible polymers by Kroy and Frey [11,18], predicting  $\beta = 3/4$  and  $\gamma = 0.0518 \times kT/\zeta_\perp l_p^{1/3}$ , where  $l_p$  denotes the persistence length and  $\zeta_\perp$  denotes the effective transverse friction coefficient (per length). In general, center-of-mass diffusion and internal polymer dynamics superimpose to  $S(Q, t) = \exp\{-Q^2[Dt + (\gamma t)^\beta]\}$ . Hence using Eq. (3) the FCS correlation function of a polymer chain is finally given by

$$g_{\text{diff}}(t) = \frac{1}{N} \frac{1}{1 + X} \frac{1}{\sqrt{(1 + \frac{1}{f^2}X)}} \quad (4)$$

with

$$X = \frac{t}{\tau_{\text{D}}} + \left(\frac{t}{\tau_{\text{C}}}\right)^\beta \quad \text{and} \quad \tau_{\text{C}} = \frac{(0.25r_0^2)^{1/\beta}}{\gamma}. \quad (5)$$

Figure 2 shows FCS correlation data taken as a function of label density  $\sigma$ , between  $1/150$  and  $1/8000 \text{ bp}^{-1}$ . Evaluation of the data reveals three separated decay times, which differ by more than 1 order of magnitude. We find a diffusive mode at long times, and at the shortest times one may identify the triplet decay. In addition, we observe a decay mode in the microsecond range, which systematically increases in amplitude and decay time with decreasing  $\sigma$ . We attribute the midrange decay to chromophore blinking, an on-off process that is introduced in the following.

It is known that the chromophore TOTO has a considerably higher binding constant than ethidium bromide,

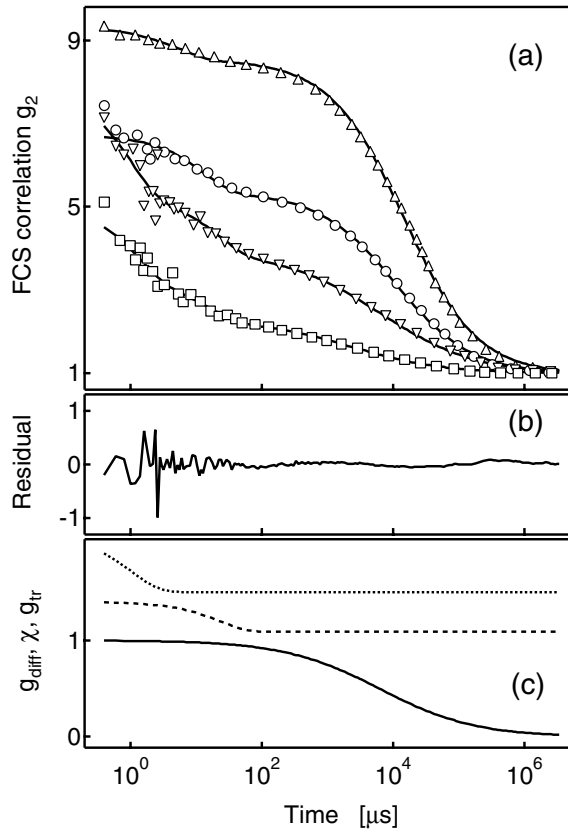


FIG. 2. Comparison of experimental correlation curves with the hydrodynamic model, corresponding to DNA label densities of 1/150, 1/500, 1/1000, and 1/8000 bp<sup>-1</sup> (top to bottom). The solid lines represent fits to Eq. (6). (b) Demonstration of residuals (from third data set). (c) Fitted dynamic contributions  $g_{\text{diff}}$  (solid line),  $\chi$  (dashed line), and  $g_{\text{tr}}$  (dotted line) for the third data set. The functions are offset for presentational purposes.

which was studied earlier [4]. We therefore assume that TOTO can be quenched in a bound state described by local on-off fluctuations  $\chi[k_{\text{off}}, K, M](t)$ . The subchain within the focus carries  $M \propto \sigma$  markers, and  $i$  of them ( $0 < i < M$ ) are emitting light at a given time. This situation is referred to by the state  $[i]$ . The local on-off dynamics may then be modeled as a birth-and-death process (BDP) [19], defined by a transfer rate  $k_{\text{on}}$  from state  $[i]$  to state  $[i + 1]$ , and a rate  $k_{\text{off}}$  to state  $[i - 1]$ . Both rates are taken to be site independent. For  $i = 0$  or  $i = M$ , the process is restricted to only one direction. Given an equilibrium probability  $\bar{P}_i$  for state  $[i]$  to occur at time  $t = 0$ , the  $S_{ik}(t)$  denote the average probability for state  $[k]$  to occur at time  $t$ . The BDP may be formalized as  $\frac{d}{dt} S_{ik}(t) = \sum_{j=1}^M T_{ij} S_{jk}(t)$  with a proper choice of the transfer rates  $T_{ij}$ . Solving this set of differential equations under the constraint  $S_{ik}(0) = \bar{P}_i \delta_{ik}$ , we calculate  $\chi[k_{\text{off}}, K, M](t) = \sum_{i,j=1}^M ij S_{ij}(t) / \sum_{i=1}^M i^2 \bar{P}_i$  with  $K = k_{\text{on}}/k_{\text{off}}$  [13]. To illustrate the behavior of  $\chi$ , we note that in the limit of a single dye it is given by  $\chi(t) = (K + 1)^{-1} \{K + \exp[-k_{\text{off}}(K + 1)t]\}$ . As the number of

dyes in the focus increases,  $\chi$  becomes a superposition of exponentials. The decay time  $k_{\text{off}}^{-1}$  decreases, and the amplitude depends on  $K$  and  $M$ .

In summary, the expression for the FCS correlation function that was used to fit the data reads

$$g_2(t) = 1 + g_{\text{tr}}[\tau_{\text{T}}, T] \chi[k_{\text{off}}, K, M] g_{\text{diff}}[N, \tau_{\text{D}}, \tau_{\text{C}}, \beta](t). \quad (6)$$

The function  $g_{\text{diff}}$  entails the diffusive number fluctuations depending on the particle number,  $N$ , the characteristic diffusion time, and the model-dependent exponent,  $\beta$ . Least-squares fits to Eq. (6) are shown as the solid lines in Fig. 2(a). For each label density,  $M$  is fixed as calculated, and together with the fitted  $K \approx 1$  determines the relative decay amplitude.  $\tau_{\text{D}}$  was fixed using  $D = 0.47 \mu\text{m}^2 \text{s}^{-1}$ , while the fitted quantities  $k_{\text{off}}$  and  $\tau_{\text{C}}$  set the time scales, and  $\beta$  is the shape of the diffusive decay. The triplet decay characterized by  $T$  and  $\tau_{\text{T}}$  is roughly independent of label density and is of no further significance (data not shown). Since we use seven parameters to fit the data, it is important to note that the characteristic time scales of the three functions  $g_{\text{tr}}$ ,  $\chi$ ,  $g_{\text{diff}}$  are well-separated processes over a time range of more than 6 orders of magnitude, as is illustrated in Fig. 2(b). The largest deviations of the best fits are typically found in the crossover regions between the decay processes.

The diffusive part of the correlation function yields a dependence of the decay time  $\tau_{\text{C}}$  on the average curvilinear label distance  $\Delta = \sigma^{-1}$ . Figure 3(a) shows the decay time to drop from  $\tau_{\text{C}} \approx 15$  ms to about 1.7 ms. At the same time, the stretching exponent  $\beta$  shown in Fig. 3(b) drops from about 0.75, which is close to the predicted value  $3/4$  [11,20] for semiflexible chains to  $0.57 \pm 0.03$  slightly lower than the Zimm value for the limit of widely spaced chromophores. A quantitative comparison of the measured diffusion times with the theory of semiflexible chains may be obtained as follows. The transverse friction coefficient per length for cylinders with diameter  $a$  is given by  $\zeta_{\perp} = 4\pi\eta / \ln(\Delta/a)$ , where  $\Delta$  usually denotes the hydrodynamic screening length. We

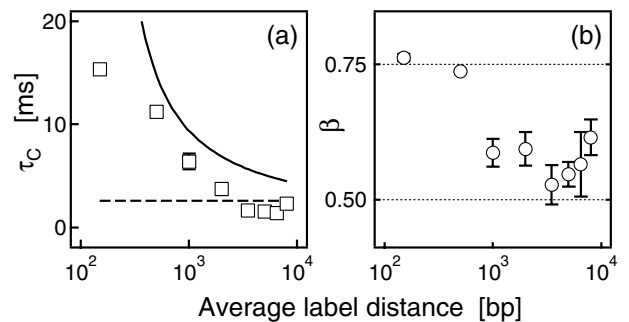


FIG. 3. (a) Diffusion time  $\tau_{\text{C}}$  vs average label distance,  $\Delta$ . The solid line indicates the semiflexible chain model, the dashed line the Zimm model. (b) Measured stretching exponent  $\beta$  vs  $\Delta$ .

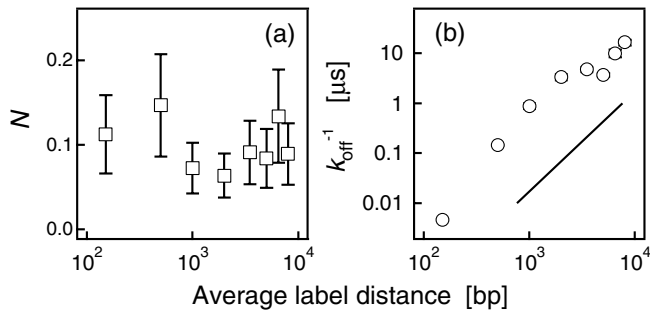


FIG. 4. (a) Number of molecules  $N$  per focal volume vs the average label distance,  $\Delta$ . (b) Reciprocal off rates,  $k_{\text{off}}^{-1}$  vs  $\Delta$ . The straight line represents a slope of 2.

identify  $\Delta$  as the average label distance, which sets the characteristic length scale. With a persistence length of 50 nm for native DNA, we estimate from [10] that one label every 150 bp will yield an increase in persistence length by at most 2%. In summary there remains no adjustable parameter and Fig. 3(a) shows the theory as a solid line in fair agreement with experiment.

An important consistency check is the number of DNA molecules  $N$  in the focal volume, which is kept constant in the experiment and determined from the autocorrelation amplitude as shown in Fig. 4(a). Because of the fact that extremely dilute solutions were used, the values obtained from best fits to Eq. (4) had to be corrected for background noise as described in Ref. [21]. The fact that  $N$  is independent of label density demonstrates that the chromophores are linked together.

The resulting parameters for the BDP,  $\chi(t)$ , clearly describe a process much faster than diffusion. Figure 4(b) shows that the corresponding time scale exhibits a remarkable dependence on the label distance, indicating  $k_{\text{off}}^{-1} \propto \Delta^2$ . The molecular interpretation of this phenomenon remains open for further investigations. A possible cause could be diffusive relaxation along the chain due to torsional modes. In this case a quenching distortion would propagate with time  $\tau_{\text{segm}} \simeq 0.5D_{\text{lin}}^{-1}\Delta^2$ , leading to  $k_{\text{off}} \propto \Delta^{-2}$  and  $D_{\text{lin}} \simeq (4.2 \pm 0.3) \mu\text{m}^2 \mu\text{s}^{-1}$ .

In conclusion our data support the picture that number density fluctuations of chromophores linked to a linear semiflexible chain can be described by a hydrodynamic model of the wormlike chain. For chains with  $R_g$  much smaller than  $r_0$  the translational mode provides the only observable FCS decay time. By contrast, chains with  $R_g$  larger than  $r_0$  exhibit FCS correlation times characterized by internal modes. Their contribution is determined by the average label density along the chain. A more dilute labeling enhances the short-wavelength modes. The observed stretching exponents derived from classical dynamic structure factors are consistent with this model and reflect the dynamics expected for semiflexible chains [11] at short distances. We emphasize that FCS proves to be a novel quantitative tool for studying macromolecular dynamics with some distinct advantages over more classical techniques. FCS is selectively sensitive to the self-

correlation part of a molecular motion. Hence FCS is complementary to coherent dynamic light scattering. Our work shows that even though FCS does not yield  $Q$ -dependent information, the intrinsic dynamic scaling of the system investigated is observable in anomalous exponents. Compared to incoherent neutron scattering, which has been widely used to study polymer dynamics, it must be noted that FCS is restricted to relatively slow motions of micron size macromolecules. In this time window, however, many biologically relevant transport problems of macromolecules in complex environments should be studied in the future.

This work is supported by the Max Planck Institute for Polymer Research and is partially supported by the DFG under Grant No. SFB 563-A4.

- [1] M. Eigen and R. Rigler, Proc. Natl. Acad. Sci. U.S.A. **91**, 5740 (1994).
- [2] R. Rigler, P. Grasselli, and M. Ehrenberg, Phys. Scr. **19**, 486 (1979).
- [3] N. G. Walter, P. Schwille, and M. Eigen, Proc. Natl. Acad. Sci. U.S.A. **93**, 12 805 (1996).
- [4] D. Magde, E. Elson, and W.W. Webb, Phys. Rev. Lett. **29**, 705 (1972).
- [5] P. Cluzel, M. Surette, and S. Leibler, Science **287**, 1652 (2000).
- [6] J. Rička and T. Binkert, Phys. Rev. A **39**, 2646 (1989).
- [7] K. Starchev, J. Zhang, and J. Buffle, J. Colloid Interface Sci. **203**, 189 (1998).
- [8] B. A. Scalettar, J.E. Hearst, and M.P. Klein, Macromolecules **22**, 4550 (1989).
- [9] S. Sukhishvili, Y. Chen, J.D. Müller, E. Gratton, K.S. Schweizer, and S. Granick, Nature (London) **406**, 146 (2000).
- [10] D.E. Smith, T.T. Perkins, and S. Chu, Macromolecules **29**, 1372 (1996).
- [11] K. Kroy and E. Frey, Phys. Rev. E **55**, 3092 (1997).
- [12] D. Magde, E. L. Elson, and W.W. Webb, Biopolymers **13**, 29 (1974).
- [13] J. Widengren, in *Fluorescence Correlation Spectroscopy*, edited by R. Rigler and E.S. Elson (Springer, Berlin, 2001), pp. 276–301.
- [14] J.S. Higgins and H.C. Benoît, *Polymers and Neutron Scattering* (Clarendon Press, Oxford, 1994).
- [15] G.R. Strobl, *The Physics of Polymers* (Springer, Berlin, 1996).
- [16] W. Brown, *Dynamic Light Scattering* (Clarendon Press, Oxford, 1993).
- [17] M. Doi and S.F. Edwards, *The Theory of Polymer Dynamics* (Oxford University Press, Oxford, 1986).
- [18] K. Kroy and E. Frey, in *Scattering in Polymeric and Colloidal Systems*, edited by W. Brown and K. Mortensen (Taylor and Francis, London, 2000).
- [19] N.G. Van Kampen, *Stochastic Processes in Physics and Chemistry* (North-Holland, Amsterdam, 1992).
- [20] R. Götter, K. Kroy, E. Frey, M. Barmann, and E. Sackmann, Macromolecules **29**, 30 (1996).
- [21] D.E. Koppel, Phys. Rev. A **10**, 1938 (1974).